Small Cell Carcinoma

7

James G. Ravenel

Small cell lung carcinoma (SCLC) is an aggressive neoplasm of neuroendocrine cell origin with a distinct biologic behavior and is therefore grouped separately from other primary lung neoplasms. SCLC represents about 15–25 % of all lung cancers and tends to occur in younger patients than those with the other lung cancers. SCLC mostly originates in the submucosa of proximal airways such as the lobar bronchi or main bronchi while a small percentage (<5 %) originates in the peripheral areas of the lung. The tumor itself is highly cellular and has a limited fibrotic or inflammatory response. Consequently, the tumor spreads rapidly through the lymphatics and blood vessels at an early stage, resulting in early nodal and distant metastatic deposits [1, 2]. From a practical standpoint, SCLC may be thought of as a "systemic" disease at the time of diagnosis.

Extrathoracic non-metastatic manifestations, or the paraneoplastic syndromes (PNS), are more common in SCLC than in NSCLC. These may be in the form of endocrinopathy, neurologic dysfunction, or skin disease. While the primary tumor is in general easily visualized by conventional imaging, FDG-PET may be helpful in documenting the tumor location when there are nonspecific conventional imaging findings [3]. The most common PNS is hyponatremia of malignancy which occurs in up to 15 % of cases and may be caused by inappropriate secretion of arginine vasopressin (antidiuretic hormone) or atrial natriuretic peptide [4, 5]. Production of ectopic corticotrophin is relatively common in SCLC but results in clinical disease, Cushing syndrome, in only 2–5 % of cases [6, 7]. Hypertrophic pulmonary osteoarthropathy is distinctly uncommon in SCLC, unlike NSCLC.

Neuromuscular PNS include Eaton–Lambert myasthenic syndrome, encephalomyelitis, and cerebellar degeneration. Eaton–Lambert myasthenic syndrome results from autoantibodies against P/Q voltage-gated calcium channels resulting in proximal muscle weakness and/or autonomic symptoms including dry mouth and constipation and occurs in approximately 3 % of SCLC cases [8]. Paraneoplastic limbic encephalitis is usually associated with anti-Hu antibody. Symptoms include psychiatric manifestations such as hallucinations, agitation, anxiety, or depression as well as memory loss, confusion, or seizures. Cerebellar degeneration has also been associated with SCLC and is manifest by ataxia, nystagmus, and dysarthria [9]. Still, the most common cause of neurological symptoms in a patient with SCLC is brain metastasis. The imaging features of PNS will be discussed later.

J.G. Ravenel, M.D. (✉)
Department of Radiology, Medical University of South Carolina, 96 Jonathan Lucas St, Room 211, P.O. Box 250322, Charleston, SC 29425, USA
e-mail: ravenejg@musc.edu

J.G. Ravenel (ed.), *Lung Cancer Imaging*, Contemporary Medical Imaging,
DOI 10.1007/978-1-60761-620-7_7,

Staging

Historically, SCLC was stratified by a two-stage system developed by the Veterans Administration Lung Cancer Study Group [10]. Limited-stage disease included disease confined to the chest and supraclavicular nodes that can be contained within a single, tolerable radiation port. The definition of limited disease was further refined by the International Association of the Study of Lung Cancer (IASLC) to state that the classification of limited SCLC should include patients with the disease restricted to one hemithorax with regional lymph node metastases, including ipsilateral hilar, ipsilateral and contralateral mediastinal, ipsilateral and contralateral supraclavicular, and ipsilateral pleural effusion independent of cytology [11].

As a practical rule, SCLC that would encompass stages I–IIIB under the current TNM system can be characterized as limited disease. Extensive stage disease included all lesions not characterized as limited stage and those with distant metastases analogous to stage IV. About 70 % of patients with SCLC present with extensive disease, and only 30 % have disease limited to the thorax. One group reported 2-year survival rates of about 10 % for limited disease and about 3 % for extensive disease. Extensive disease with only brain metastasis may have a survival rate similar to that of limited disease.

A relatively large retrospective series suggested that 5-year survival was enhanced (37.1 %) with surgery (the majority diagnosed prior to surgery) for pathologic stages IA–IIB, and survival was further improved with the addition of at least four cycles of chemotherapy to surgery [12]. Based on further analysis of resected SCLCs, the IASLC has found sufficient prognostic variability using the TNM system to warrant replacing the previous staging system [13]. For surgically resected SCLC ($n=349$), there is a marked survival enhancement (>2 years) for both stage T1a and N0 cases compared with other surgically resected SCLCs [13]. Moreover, 5-year survival for resected stage I tumors is 57 %. Unfortunately, comparisons with standard chemoradiotherapy are difficult since complete TNM pathologic staging is unavailable for nonsurgical cases and nonsurgical cases are traditionally labeled as limited disease and also biased toward higher TNM stages. Given these limitations, the overall 5-year survival for all surgically resected "limited disease" is 34.5 % and favorable compared to the 12–25 % for traditional chemoradiotherapy [1]. It should be noted that surgically resected cases account for only 3 % of all SCLC cases. The survival differences across pathologically staged SCLC are considered sufficient to warrant using the TNM system to stratify patients for treatment trials rather than the prior limited/extensive classification, although for clinical purposes outside of therapeutic trials the relatively simple limited/extensive classification probably is sufficient to guide treatment.

Imaging of Small Cell Lung Cancer

Imaging Chest and Abdomen

Because of the predilection for early metastatic spread, the primary site is often not visible by conventional radiography or CT. The typical primary site is radiographically occult submucosal endobronchial lesion that subsequently metastasizes to the mediastinal and hilar lymph nodes resulting in detection and the usual radiographic presentation of a large hilar and/or mediastinal mass (Fig. 7.1) [1]. Approximately 4 % of lung cancers presenting as a solitary pulmonary nodule (SPN) turn out to be SCLC (Fig. 7.2) and approximately 4 % of small cell cancers of the lung will present as an SPN [14]. There are no imaging features that otherwise distinguish SCLC and NSCLC when presenting as an SPN.

The mediastinum is by far the most common site of detected disease and varies in series from 66 to 92 % of cases [1, 15]. The mediastinal mass may grow so large that it obstructs the superior vena cava (SVC) (Fig. 7.3). SVC syndrome is a clinical diagnosis based on generalized swelling of the upper limbs, neck, and face associated with a mediastinal or paramediastinal lesion. Tumor growth in the mediastinum may also be associated

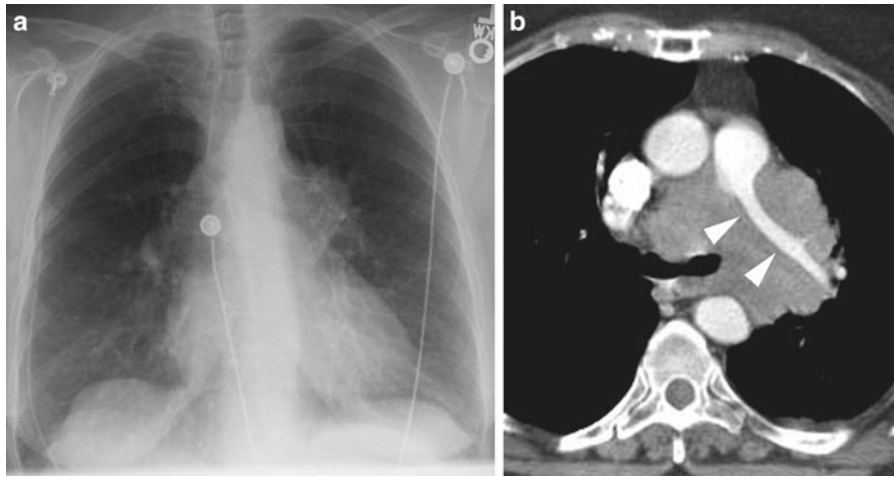

Fig. 7.1 Typical radiographic appearance of small cell lung cancer. (**a**) Frontal radiograph reveals mass involving the left hilum and aorto-pulmonary window without discrete parenchymal lesion. (**b**) Contrast-enhanced CT confirms mass as well as shows attenuation and narrowing of the left pulmonary artery (*arrowheads*)

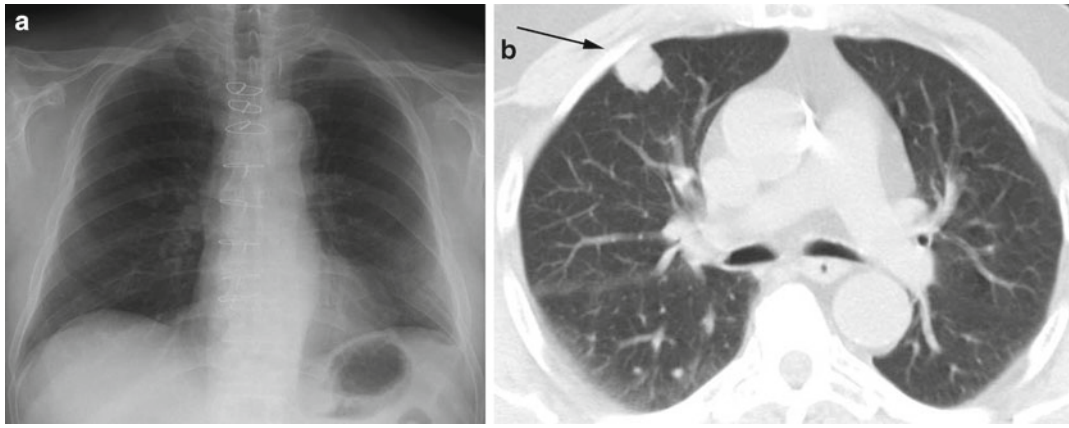

Fig. 7.2 (**a**, **b**) Small cell carcinoma (SCLC) presenting as a solitary pulmonary nodule (SPN). CT reveals slightly lobulated right upper lobe nodule (*arrow*). There are no radiographic features by which to differentiate from non-small cell lung cancers

with dyspnea, hoarseness, and dysphagia. In up to12 % of cases of SCLC, SVC syndrome is present at the time of initial diagnosis [4]. Invasion of the pericardium (38 %) and narrowing of central bronchi (68 %) can also occur and be detected with CT (Fig. 7.4) [3].

Once the tumor has access to the mediastinum, there are pathways of spread into the abdomen via the aortic and esophageal hiatus and into the neck. This can result in intra-abdominal lymphadenopathy primarily along the celiac vessels resulting in celiac, periportal (Fig. 7.5), and peripancreatic adenopathy. Previous studies show the incidence of disease in the peripancreatic and retroperitoneal lymph nodes to be 6 % [6]. Disease may also reach the gastrohepatic ligament either by spread along vascular planes or through the esophageal hiatus. Spread into the

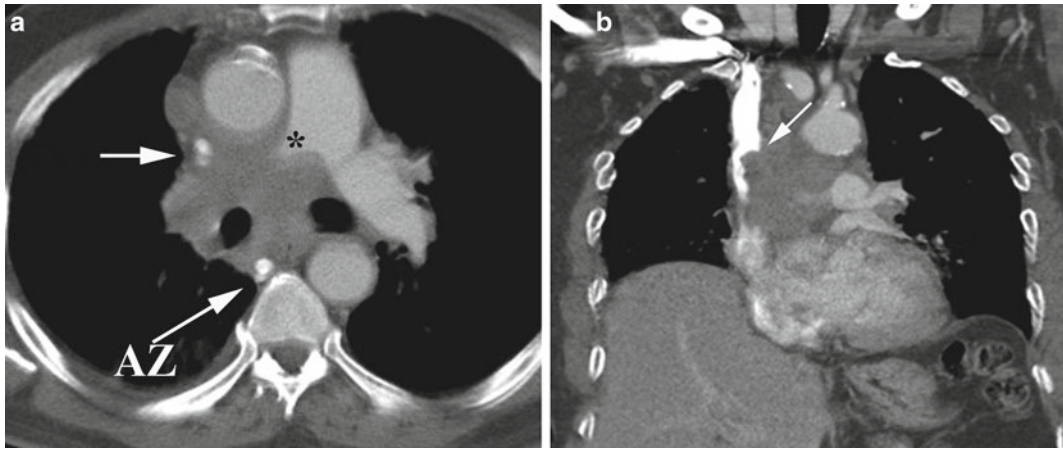

Fig. 7.3 Superior vena cava (SVC) obstruction. (**a**) Axial CT image reveals large mass surrounding and narrowing the SVC (*arrow*) as well as obstructing the right pulmonary artery (*asterisk*). Note collateral retrograde venous flow through the azygous vein (*AZ*). (**b**) Coronal reformation shows the mass invading the medial wall of the SVC (*arrow*)

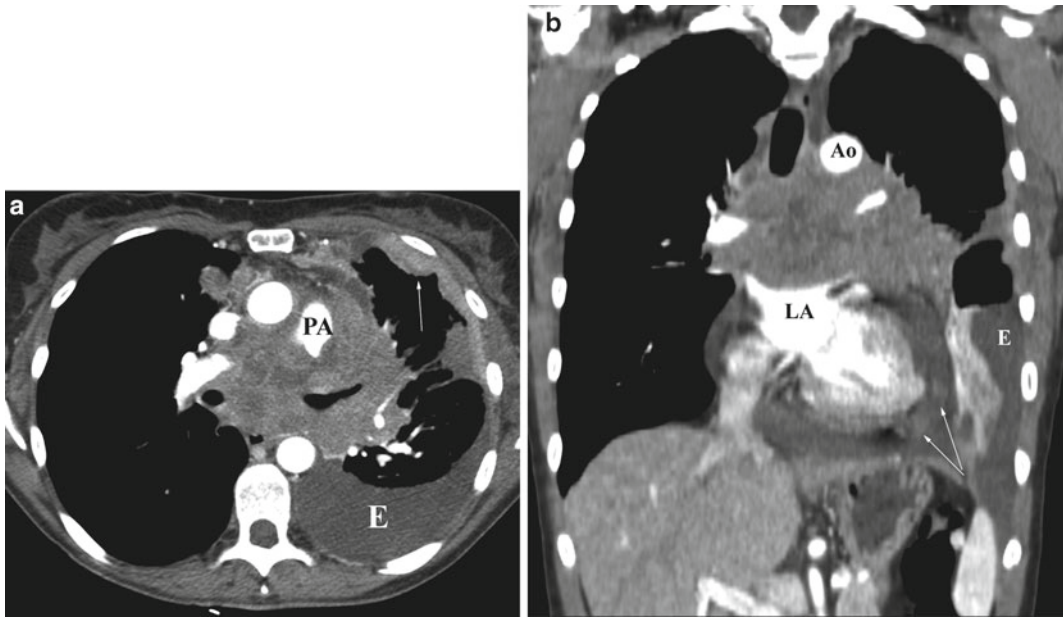

Fig. 7.4 SCLC with pleural and pericardial metastases. (**a**) Axial CT image reveals large mass infiltrating the mediastinum and markedly narrowing the origin of the left pulmonary artery (*PA*). There is associated left pleural effusion (*E*) with metastatic pleural implants anteriorly (*arrow*). (**b**) Coronal reformation reveals mass effect on the transverse aorta (*Ao*) and left atrium (*LA*) as well as a pericardial effusion with two discrete pericardial nodules (*arrow*) and left pleural effusion (*E*)

neck via the cervicothoracic continuum can result in ipsilateral supraclavicular adenopathy.

A majority of patients will have distant metastatic disease at presentation with up to 60 % having metastatic disease in the abdomen at the time of diagnosis. The adrenal gland and liver are the most frequent sites of disease (Figs. 7.6 and 7.7), although any abdominal organ can be affected

Fig. 7.5 Periportal adenopathy. Axial CT image reveals enlarged lymph nodes in the porta hepatis (*arrows*) surrounding common hepatic artery from SCLC

Table 7.1 Sites of metastatic disease

Site	% Involved at presentation	% Involved at autopsy
Mediastinal nodes	66–92	73–87
Bone	27–41	54
Liver	21–27	69
Adrenal	5–31	35–65
CNS	10–14	28–50
Retroperitoneal nodes	3–13	29–52
Supraclavicular nodes	17	42
Pleural effusion	16–20	30
Contralateral lung	1–12	8–27
Soft tissue	5	19

Adapted from Jackman DM, Johnson BE. Small-cell lung cancer. Lancet 2005;366(9494):1385–96

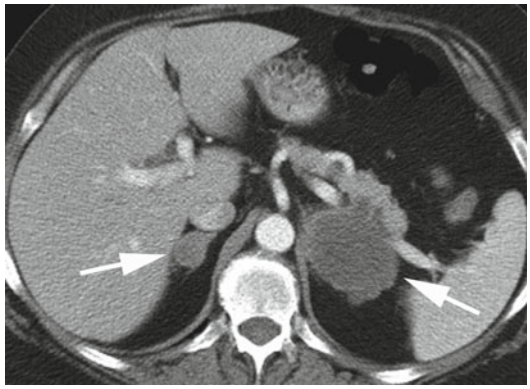

Fig. 7.6 Adrenal metastases. Axial CT image reveals necrotic low attenuation adrenal metastases (*arrows*)

Fig. 7.7 Hepatic metastases. Axial CT image reveals multiple low attenuation nodules within the hepatic parenchyma

[16, 17] (Table 7.1). Because of this high frequency, a CT of the abdomen with contrast is considered indicated as part of routine staging [18].

Imaging of CNS in SCLC

Due to the high incidence of brain metastases, routine imaging of the central nervous system (CNS) is warranted. Cerebral metastases have been said to be present in up to 10 % of individuals at the time of diagnosis [19, 20]. The use of routine MR of the brain has resulted in a higher incidence and number of detected brain metastases, particularly in the neurologically asymptomatic patients [21]. PET/CT is generally not helpful for detection of cerebral metastases in SCLC regardless of the level of activity in the primary tumor [22]. While important for staging and treatment planning, it is unclear that early detection of asymptomatic cerebral metastases results in improved survival [18, 23]. The typical imaging appearance of a brain metastasis is a single or multiple rim-enhancing lesions (Fig. 7.8). If small the entire lesion may show homogeneous contrast enhancement. These lesions are, in general, easily distinguished for paraneoplastic lesions. For example, PLE will show high signal in the medial temporal lobe on FLAIR or T2-weighted images (Fig. 7.9), while cerebellar degeneration may be manifest early by transient

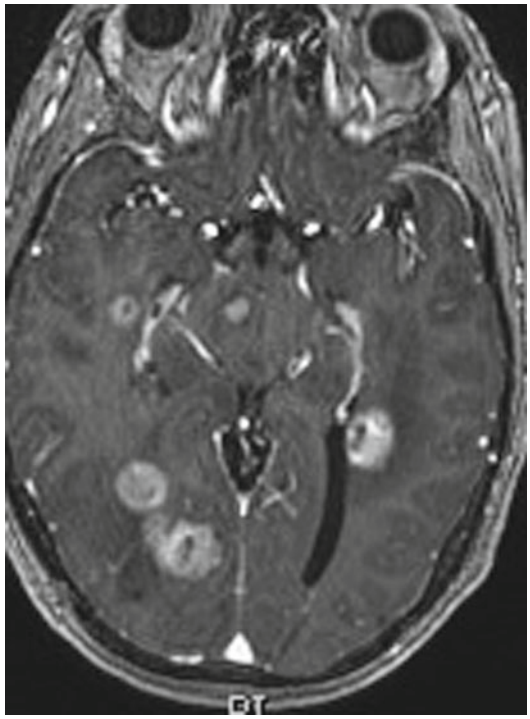

Fig. 7.8 Cerebral metastases. Axial gadolinium-enhanced T1-weighted image reveals multiple enhancing brain lesions with surrounding low signal vasogenic edema in the cerebrum and pons

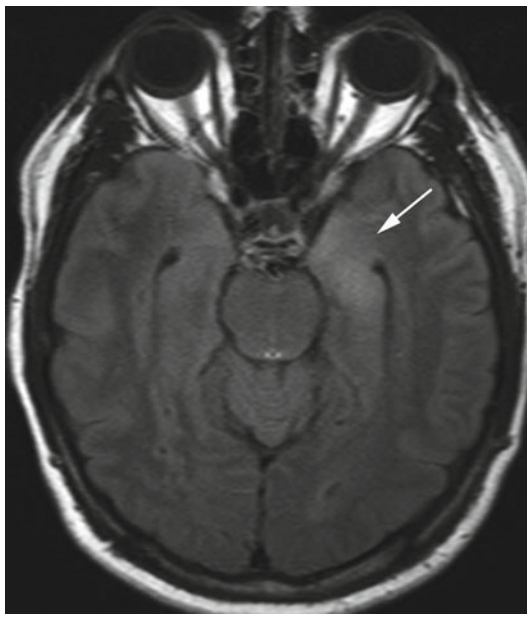

Fig. 7.9 Paraneoplastic limbic encephalitis. Axial FLAIR image reveals faintly increased signal in the left temporal lobe (*arrow*)

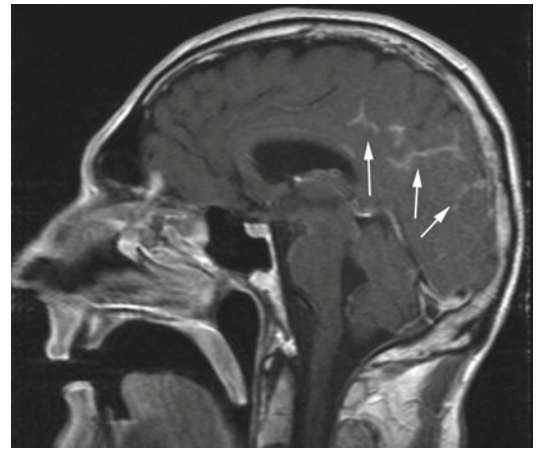

Fig. 7.10 Leptomeningeal carcinomatosis. Sagittal gadolinium-enhanced T1-weighted image reveals meningeal enhancement along the sulci of the posterior cerebral cortex (*arrows*)

enlargement of the cerebellum and meningeal enhancement and late by cerebellar atrophy [24]. Leptomeningeal disease is rare occurring in <2 % of cases (Fig. 7.10) [25].

Imaging of Osseous Metastases

Bone is considered to be the most common site of metastatic disease overall (35 % of cases), and therefore bone scintigraphy is generally part of the initial staging evaluation [26]. A whole body technique, bone scintigraphy detects signs of osseous repair, thus uptake is nonspecific and can be seen in healing fractures, degenerative joint, or spine disease as well as metastatic lesions. For the indeterminate lesion on bone scintigraphy, MR is useful to determine the etiology of the increased uptake. As data accumulates in other malignancies as well as SCLC, it is likely that bone scintigraphy will be replaced in the imaging algorithm by whole body PET/CT. Historically, bilateral bone marrow biopsies or aspirations were also suggested during initial staging, since this may be the only site of metastatic disease and detection would result in a change of stage from limited to extensive. This has been abandoned given the very low incidence of marrow disease in the absence of obvious disease on conventional imaging [18].

FDG-PET/CT

Staging

PET/CT has the potential to provide more accurate staging and prognostic information compared with conventional staging (Fig. 7.11) changing management in up to 25 % of patients, although studies remain limited to relatively small retrospective series [27]. The major value lies in the ability of PET/CT to upstage patients to extensive disease and spare the patient unnecessary therapy. Small cases series show that patients are upstaged in 8–15 % of cases as well as downstaged from extensive to limited disease in 5–10 % [28–31]. In a prospective trial PET/CT was shown to be superior to a conventional staging regimen of CT, bone scintigraphy, and bone marrow analysis, changing stage in 5 of 29 (17 %) subjects [29].

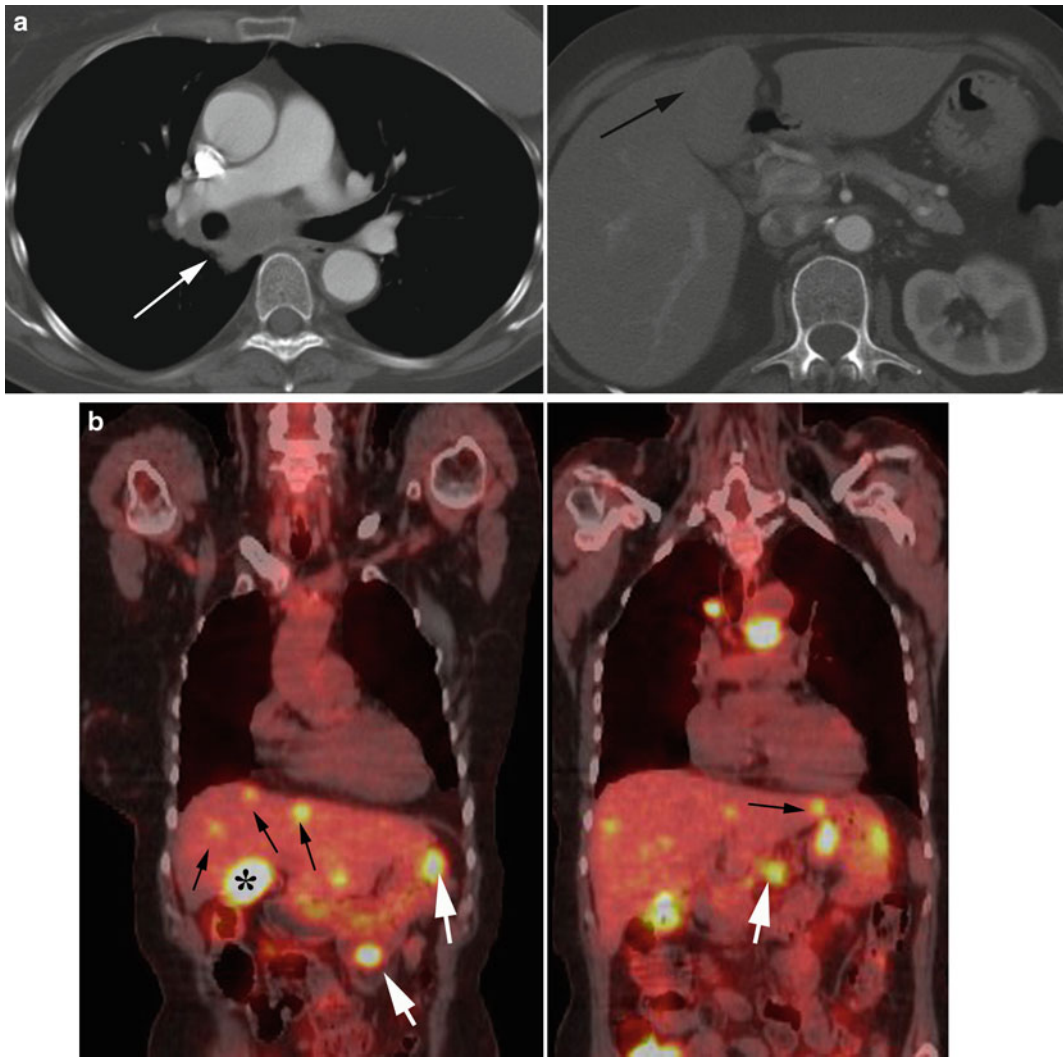

Fig. 7.11 Value of FDG-PET/CT in assessing extent of disease. (**a**) Axial CT images reveal mediastinal adenopathy and solitary hepatic metastasis (*arrows*) as the only sites of disease on conventional staging. (**b**) Coronal FDG-PET/CT images confirm the adenopathy and liver metastasis (*asterisk*) but reveal multiple additional liver metastases (*black arrows*) as well as multiple metastatic nodules in mesentery adjacent to bowel and stomach walls (*white arrows*)

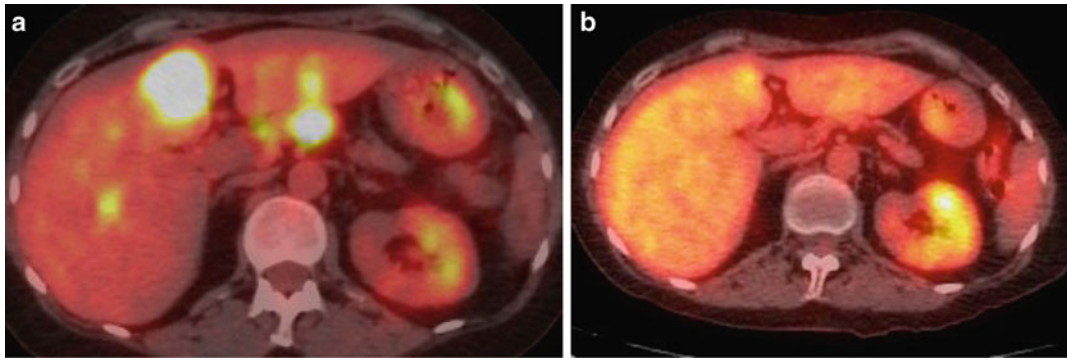

Fig. 7.12 Value of FDG-PET/CT in restaging. (**a**) Axial FDG-PET/CT shows multiple hepatic metastases. (**b**) After four cycles of chemotherapy, only dominant lesion remains metabolically active and has decreased from SUV of 10.4 to 3.6

Treatment Planning

In patients treated with radiation therapy, the field size has important implications both in terms of toxicity and possibility of local failure. The addition of FDG-PET to usual staging allows for better delineation of treatment fields through both the inclusion of otherwise unsuspected sites or exclusion of unaffected nodal stations. This may result in adjustment of the radiation therapy plan in up to 30 % of cases [31–33]. Because of respiratory artifact, it is ultimately incumbent on evaluating sites of uptake based and gross tumor volume based on the CT component to ultimately determine the tumor outline. The effect of such approach is the elimination of elective nodal irradiation with the presumed benefit of higher delivery of radiation to the clinical tumor volume (CTV). It is important to note that such an approach is associated with approximately 10 % rate of nodal recurrence outside of the CTV [33–35], although isolated nodal failure (that without associated distant disease) was 3 % in the study by van Loon.

Prognosis

Other potential uses of PET/CT in SCLC including determination of prognosis and response to therapy remain uncertain [36, 37]. Similar to non-small cell lung cancer, a higher SUV is associated with a poorer prognosis. Using the median SUVmax (8.7) as a cutoff in a cohort of 76 patients, stage-specific survival was increased 15 months for limited disease and 8 months for extensive disease for those with median SUVmax below the median [38]. With regard to post-therapeutic staging, in a retrospective review of 22 subjects using FDG-PET, a post-therapy negative PET was a better predictor of overall survival compared with non-metabolic responders (Fig. 7.12). In addition, metabolic response was a better predictor than anatomic response (Fig. 7.13) [39]. Another small study including 25 subjects suggested that post-therapy PET alters management in approximately 50 %. Unfortunately over 80 % of cases in that study did not have a pretreatment PET for comparison [40]. The utility of FDG-PET as an imaging biomarker in SCLC awaits further confirmation.

Conclusion

Although apparently decreasing in incidence, small cell lung cancer remains associated with a poor prognosis often due to distant metastatic disease at the time of diagnosis. The staging paradigm has shifted to a TNM classification so that appropriate patients may be considered for surgery. The radiologic staging has also changed from a multi-modality approach to one using predominately PET/CT as well as imaging of the brain, preferably MR imaging.

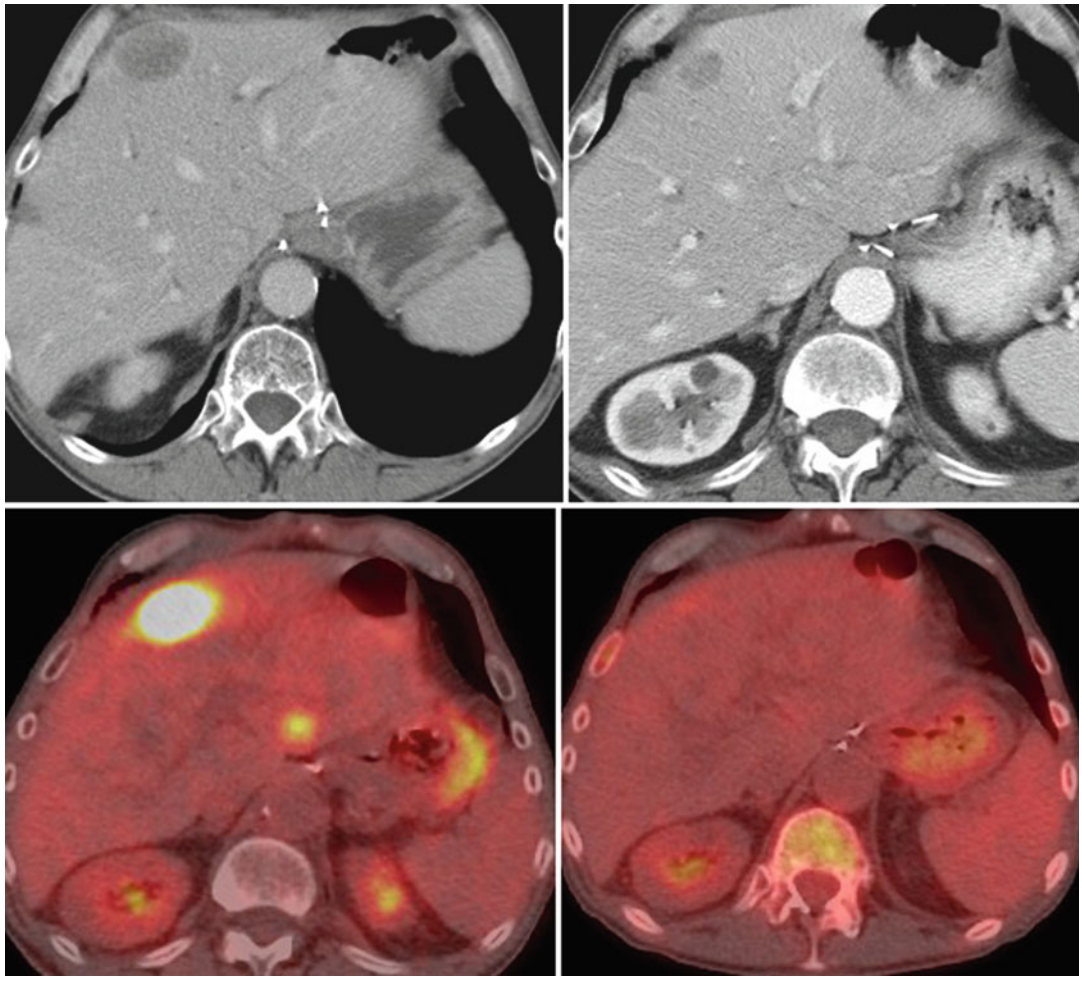

Fig. 7.13 Value of FDG-PET in restaging. Composite image of CT and FDG-PET/CT at two different time points. CT images reveal a decrease in diameter of 50 % which would be termed a partial response to therapy. PET/CT images however reveal a complete metabolic response even with a persistent anatomic abnormality

References

1. Jackman DM, Johnson BE. Small-cell lung cancer. Lancet. 2005;366(9494):1385–96.
2. Sher T, Dy GK, Adjei AA. Small cell lung cancer. Mayo Clin Proc. 2008;83(3):355–67.
3. Crotty E, Patz Jr EF. FDG-PET imaging in patients with paraneoplastic syndromes and suspected small cell lung cancer. J Thorac Imaging. 2001;16(2):89–93.
4. Campling BG, Sarda IR, Baer KA, et al. Secretion of atrial natriuretic peptide and vasopressin by small cell lung cancer. Cancer. 1995;75(10):2442–51.
5. Johnson BE, Chute JP, Rushin J, et al. A prospective study of patients with lung cancer and hyponatremia of malignancy. Am J Respir Crit Care Med. 1997;156(5):1669–78.
6. Shepherd FA, Laskey J, Evans WK, Goss PE, Johansen E, Khamsi F. Cushing's syndrome associated with ectopic corticotropin production and small-cell lung cancer. J Clin Oncol. 1992;10(1):21–7.
7. Stewart PM, Gibson S, Crosby SR, et al. ACTH precursors characterize the ectopic ACTH syndrome. Clin Endocrinol (Oxf). 1994;40(2):199–204.
8. Seute T, Leffers P, ten Velde GP, Twijnstra A. Neurologic disorders in 432 consecutive patients with small cell lung carcinoma. Cancer. 2004;100(4):801–6.
9. Toothaker TB, Rubin M. Paraneoplastic neurological syndromes: a review. Neurologist. 2009;15(1):21–33.
10. Osterlind K, Ihde DC, Ettinger DS, et al. Staging and prognostic factors in small cell carcinoma of the lung. Cancer Treat Rep. 1983;67(1):3–9.

11. Stahel R, Ginsberg R, Havemann K, et al. Staging and prognostic factors in small cell lung cancer: a consensus report. Lung Cancer. 1989;5:119–26.
12. Inoue M, Miyoshi S, Yasumitsu T, et al. Surgical results for small cell lung cancer based on the new TNM staging system. Thoracic Surgery Study Group of Osaka University, Osaka, Japan. Ann Thorac Surg. 2000;70(5):1615–9.
13. Vallières E, Shepherd FA, Crowley J, et al. The IASLC Lung Cancer Staging Project: proposals regarding the relevance of TNM in the pathologic staging of small cell lung cancer in the forthcoming (seventh) edition of the TNM classification for lung cancer. J Thorac Oncol. 2009;4(9):1049–59.
14. Kreisman H, Wolkove N, Quoix E. Small cell lung cancer presenting as a solitary pulmonary nodule. Chest. 1992;101(1):225–31.
15. Pearlberg JL, Sandler MA, Lewis Jr JW, Beute GH, Alpern MB. Small-cell bronchogenic carcinoma: CT evaluation. AJR Am J Roentgenol. 1988;150(2): 265–8.
16. Whitley NO, Mirvis SE. Abdominal CT in the staging of small cell carcinoma of the lung. Crit Rev Diagn Imaging. 1989;29(2):103–16.
17. Mirvis SE, Whitley NO, Aisner J, Moody M, Whitacre M, Whitley JE. Abdominal CT in the staging of small-cell carcinoma of the lung: incidence of metastases and effect on prognosis. AJR Am J Roentgenol. 1987;148(5):845–7.
18. Simon GR, Turrisi A, American College of Chest Physicians. Management of small cell lung cancer: ACCP evidence-based clinical practice guidelines (2nd edition). Chest. 2007;132(3 Suppl):324S–39S.
19. Hirsch FR, Paulson OB, Hansen HH, Larsen SO. Intracranial metastases in small cell carcinoma of the lung. Prognostic aspects. Cancer. 1983;51(3): 529–33.
20. Giannone L, Johnson DH, Hande KR, Greco FA. Favorable prognosis of brain metastases in small cell lung cancer. Ann Intern Med. 1987;106(3):386–9.
21. Seute T, Leffers P, ten Velde GP, Twijnstra A. Detection of brain metastases from small cell lung cancer: consequences of changing imaging techniques (CT versus MRI). Cancer. 2008;112(8):1827–34.
22. Lee HY, Chung JK, Jeong JM, et al. Comparison of FDG-PET findings of brain metastasis from non-small-cell lung cancer and small-cell lung cancer. Ann Nucl Med. 2008;22(4):281–6.
23. Hochstenbag MM, Twijnstra A, Wilmink JT, Wouters EF, ten Velde GP. Asymptomatic brain metastases (BM) in small cell lung cancer (SCLC): MR-imaging is useful at initial diagnosis. J Neurooncol. 2000;48(3):243–8.
24. Dalmau J, Rosenfeld MR. Paraneoplastic syndromes of the CNS. Lancet Neurol. 2008;7(4):327–40.
25. Seute T, Leffers P, ten Velde GP, Twijnstra A. Leptomeningeal metastases from small cell lung carcinoma. Cancer. 2005;104(8):1700–5.
26. Adjei AA, Marks RS, Bonner JA. Current guidelines for the management of small cell lung cancer. Mayo Clin Proc. 1999;74(8):809–16.
27. Azad A, Chionh F, Scott AM, et al. High impact of 18F-FDG-PET on management and prognostic stratification of newly diagnosed small cell lung cancer. Mol Imaging Biol. 2010;12(4):443–51.
28. Niho S, Fujii H, Murakami K, et al. Detection of unsuspected distant metastases and/or regional nodes by FDG-PET [corrected] scan in apparent limited-disease small-cell lung cancer. Lung Cancer. 2007;57(3):328–33.
29. Fischer BM, Mortensen J, Langer SW, et al. A prospective study of PET/CT in initial staging of small-cell lung cancer: comparison with CT, bone scintigraphy and bone marrow analysis. Ann Oncol. 2007;18(2):338–45.
30. Brink I, Schumacher T, Mix M, et al. Impact of [18F] FDG-PET on the primary staging of small-cell lung cancer. Eur J Nucl Med Mol Imaging. 2004;31(12): 1614–20.
31. Bradley JD, Dehdashti F, Mintun MA, Govindan R, Trinkaus K, Siegel BA. Positron emission tomography in limited-stage small-cell lung cancer: a prospective study. J Clin Oncol. 2004;22(16):3248–54.
32. van Loon J, Offermann C, Bosmans G, et al. 18FDG-PET based radiation planning of mediastinal lymph nodes in limited disease small cell lung cancer changes radiotherapy fields: a planning study. Radiother Oncol. 2008;87(1):49–54.
33. van Loon J, De Ruysscher D, Wanders R, et al. Selective nodal irradiation on basis of (18)FDG-PET scans in limited-disease small-cell lung cancer: a prospective study. Int J Radiat Oncol Biol Phys. 2010; 77(2):329–36.
34. Salem A, Abuodeh Y, Khader J. Selective nodal irradiation on basis of (18)FDG-PET scans in limited-disease small-cell lung cancer: a prospective study. In regard to van Loon et al. (Int J Radiat Oncol Biol Phys 2010;77:329–336). Int J Radiat Oncol Biol Phys. 2010;78(5):1606; author reply 1606–7.
35. De Ruysscher D, Bremer RH, Koppe F, et al. Omission of elective node irradiation on basis of CT-scans in patients with limited disease small cell lung cancer: a phase II trial. Radiother Oncol. 2006;80(3):307–12.
36. Kut V, Spies W, Spies S, Gooding W, Argiris A. Staging and monitoring of small cell lung cancer using [18F]fluoro-2-deoxy-D-glucose-positron emission tomography (FDG-PET). Am J Clin Oncol. 2007;30(1):45–50.
37. Fischer BM, Mortensen J, Langer SW, et al. PET/CT imaging in response evaluation of patients with small cell lung cancer. Lung Cancer. 2006;54(1):41–9.
38. Lee YJ, Cho A, Cho BC, et al. High tumor metabolic activity as measured by fluorodeoxyglucose positron emission tomography is associated with poor prognosis in limited and extensive stage small-cell lung cancer. Clin Cancer Res. 2009;15(7):2426–32.
39. Onitilo AA, Engel JM, Demos JM, Mukesh B. Prognostic significance of 18 F-fluorodeoxyglucose—positron emission tomography after treatment in patients with limited stage small cell lung cancer. Clin Med Res. 2008;6(2):72–7.
40. Blum R, MacManus MP, Rischin D, Michael M, Ball D, Hicks RJ. Impact of positron emission tomography on the management of patients with small-cell lung cancer: preliminary experience. Am J Clin Oncol. 2004;27(2):164–71.